Molecular dissection of the photoreceptor ribbon synapse: physical interaction of Bassoon and RIBEYE is essential for the assembly of the ribbon complex

Susanne tom Dieck,[1,2] Wilko D. Altrock,[2] Michael M. Kessels,[2] Britta Qualmann,[2] Hanna Regus,[1] Dana Brauner,[1] Anna Fejtová,[2] Oliver Bracko,[2] Eckart D. Gundelfinger,[2] and Johann H. Brandstätter[1,3]

[1]Department of Neuroanatomy, Max Planck Institute for Brain Research, D-60528 Frankfurt/Main, Germany
[2]Leibniz Institute for Neurobiology, D-39118 Magdeburg, Germany
[3]Institute for Zoology, University of Erlangen-Nuernberg, D-91058 Erlangen, Germany

The ribbon complex of retinal photoreceptor synapses represents a specialization of the cytomatrix at the active zone (CAZ) present at conventional synapses. In mice deficient for the CAZ protein Bassoon, ribbons are not anchored to the presynaptic membrane but float freely in the cytoplasm. Exploiting this phenotype, we dissected the molecular structure of the photoreceptor ribbon complex. Identifiable CAZ proteins segregate into two compartments at the ribbon: a ribbon-associated compartment including Piccolo, RIBEYE, CtBP1/BARS, RIM1, and the motor protein KIF3A, and an active zone compartment including RIM2, Munc13-1, a Ca^{2+} channel α1 subunit, and ERC2/CAST1. A direct interaction between the ribbon-specific protein RIBEYE and Bassoon seems to link the two compartments and is responsible for the physical integrity of the photoreceptor ribbon complex. Finally, we found the RIBEYE homologue CtBP1 at ribbon and conventional synapses, suggesting a novel role for the CtBP/BARS family in the molecular assembly and function of central nervous system synapses.

Introduction

Chemical synapses are highly specialized cell–cell contacts that mediate efficient communication between nerve cells. Ultrastructurally, distinct pre- and postsynaptic regions mark the sites of neurotransmitter release and reception. Presynaptically, the regulated release of neurotransmitter is restricted to the active zone, which is characterized by an electron-dense cytoskeletal meshwork. This cytomatrix at the active zone (CAZ) is exactly aligned with the postsynaptic reception apparatus, an electron-dense cytoskeletal matrix known as the postsynaptic density (Ziff, 1997; Dresbach et al., 2001).

The mature CAZ is defined by a set of multidomain proteins that harbor several protein–protein or protein–lipid interaction domains. The complete protein composition of the CAZ is not known to date, but it includes the proteins Munc13-1 (Brose et al., 1995), RIMs (Wang et al., 1997, 2000), ERC/CAST (Ohtsuka et al., 2002; Wang et al., 2002), Piccolo/Aczonin, and Bassoon (Cases-Langhoff et al., 1996; tom Dieck et al., 1998; Wang et al., 1999). Piccolo and Bassoon are among the first CAZ proteins to appear at nascent synapses in cultured neurons and they are components of an active zone precursor vesicle (Vardinon-Friedman et al., 2000; Zhai et al., 2001; Shapira et al., 2003). Furthermore, they are very large multidomain proteins that are intimately anchored to the cortical actin/spectrin cytoskeleton and are present at both excitatory and inhibitory synapses in the brain (Richter et al., 1999; Wang et al., 1999; Fenster et al., 2000, 2003). This makes Piccolo and Bassoon prime candidates for scaffolding proteins involved in the assembly of functional active zones.

A unique type of chemical synapse, structurally and functionally specialized for the tonic release of neurotransmitter in the dark, is the photoreceptor ribbon synapse. The presynaptic ribbon constitutes an electron-dense band of large surface area that extends from the site of transmitter release into the presynaptic cytoplasm and is covered by hundreds of synaptic vesicles (Rao-Mirotznik et al., 1995). The synaptic ribbon was thought to be a unique structure specialized to ribbon synapses in sensory organs. However, an emerging idea is that all chemical synapses are organized according to a common principle in which structural differences correlate with the kinetics of transmitter release (Zhai and Bellen, 2004). Within this concept, every synapse has dense projections on which vesicles are tethered, and the ribbon is a variation of this common theme. The ribbon is defined

S. tom Dieck and W.D. Altrock contributed equally to this paper.
Correspondence to Johann H. Brandstätter: brandstaett@mpih-frankfurt.mpg.de
Abbreviation used in this paper: CAZ, cytomatrix at the active zone.

The Journal of Cell Biology, Vol. 168, No. 5, February 28, 2005 825–836
http://www.jcb.org/cgi/doi/10.1083/jcb.200408157

and organized by a scaffold of proteins that are just beginning to be identified. One of these proteins is RIBEYE. It has self-aggregating properties and is a major constituent of the ribbon (Schmitz et al., 2000). Another protein, the kinesin motor protein KIF3A, is enriched at ribbons, but its function there is still unknown (Muresan et al., 1999). Two other integral components of photoreceptor ribbon synapses are Bassoon and Piccolo (Brandstätter et al., 1999; Dick et al., 2001). In mouse retinae deficient for functional Bassoon protein, photoreceptor ribbons are not anchored to the presynaptic active zones, but float freely in the cytoplasm and transmitter release is greatly perturbed (Dick et al., 2003). These results demonstrated a critical role of Bassoon in the formation and function of photoreceptor ribbon synapses.

To gain a more detailed picture of the photoreceptor ribbon protein architecture, we exploited the phenotype of the Bassoon mutant mouse. We report the segregation of CAZ proteins into two distinct molecular compartments of the ribbon complex: a ribbon and an active zone compartment. The physical interaction between Bassoon and RIBEYE seems to be involved in linking the two compartments and the assembly of a functional ribbon complex. Finally, we report that the RIBEYE homologue CtBP1/BARS (COOH-terminal binding protein 1/brefeldin A adenosine diphosphate ribosylated substrate), a protein that has previously been identified as a transcription corepressor and Golgi-localized membrane-fissioning protein (Weigert et al., 1999; Turner and Crossley, 2001), is present both at photoreceptor ribbon synapses and at conventional synapses of retina and brain. This finding suggests a novel role for the CtBP family in the molecular assembly and function of central nervous system synapses.

Results

Protein composition of the presynaptic photoreceptor ribbon complex

In a retina deficient of a functional Bassoon protein, the photoreceptor ribbons are not anchored to the presynaptic membrane and float freely in the photoreceptor terminals (Dick et al., 2003). We exploited the phenotype of free-floating ribbons to screen for active zone molecules associated with the ribbon complex. As a marker for photoreceptor ribbon material we chose RIBEYE, the major protein component of photoreceptor and bipolar cell ribbons in the retina (Schmitz et al., 2000). RIBEYE is composed of a unique A-domain specific for ribbons, and a B-domain that is, with the exception of the first 20 amino acids, identical to the transcriptional corepressor CtBP2. Both RIBEYE and CtBP2 are derived from the same gene (Schmitz et al., 2000).

We generated an antiserum against the RIBEYE-specific A-domain. In retina homogenate this antiserum recognizes two protein bands of ~110 and 120 kD that are also detected with an antibody against the B-domain (Fig. 1 A). In addition, the B-domain antibody recognizes the 50-kD CtBP2 band (Fig. 1 A). In preadsorbed controls, the immunodetection of RIBEYE in Western blots and in mouse retinal sections was abolished (Fig. 1, B and D).

In vertical sections of wild-type mouse retina, the A-domain antiserum produces labeling in the two synaptic layers of the retina, the outer plexiform layer (OPL) and the inner plexiform layer (IPL) (Fig. 1 C). The labeling represents RIBEYE at the glutamatergic ribbon synapses of the photoreceptors in the OPL and the bipolar cells in the IPL. Staining with the B-domain antibody is comparable to that obtained with the A-domain antiserum. In addition, immunoreactivity in the nuclear layers of the retina is observed, which derives from staining of the transcriptional corepressor CtBP2 (unpublished data). Postembedding immunogold EM shows an identical distribution of gold particles for A- and B-domain antibodies over the whole length of the photoreceptor synaptic ribbons (Fig. 1, E and F), a result corroborated by double-labeling immunocytochemistry and confocal laser-scanning microscopy (Fig. 1 G). Of note, the region of the arciform density at the ribbon base is free of immunogold particles in both cases (Fig. 1, E and F; arrowheads). These experiments indicate that both A- and B-domain antibodies recognize the same protein at photoreceptor ribbon synapses, i.e., RIBEYE (see also Schmitz et al., 2000). That RIBEYE represents ribbon material is further demonstrated by the fact that the free-floating photoreceptor ribbons in the Bassoon mutant retina are decorated with RIBEYE immunoreactivity (Fig. 1 H). Both A- and B-domain antibodies were used interchangeably in the study to label photoreceptor ribbons.

With immunocytochemistry and confocal laser-scanning microscopy, we screened in wild-type photoreceptor terminals a number of presynaptic proteins for their localization as compared with RIBEYE and thus for their potential to interact with the photoreceptor ribbon. The proteins synaptotagmin, VGLUT1 (vesicular glutamate transporter 1), SNAP-25 (synaptosomal-associated protein of 25 kD), syntaxin 3, and synaptophysin were present throughout the photoreceptor terminals; they did not specifically colocalize with RIBEYE, and thus were excluded from further analysis (unpublished data). Proteins that colocalized with RIBEYE in wild-type photoreceptor terminals were Piccolo, the kinesin motor protein KIF3A, RIM1, RIM2, Munc13-1, a Ca^{2+} channel α1 subunit, ERC2/CAST1 (Fig. 2), and Bassoon (see Fig. 6).

In a next step, we addressed the question of whether these proteins are integral parts of the protein network of the ribbon or are associated rather with the active zone membrane. Therefore, we screened these proteins for their colocalization with RIBEYE in Bassoon mutant photoreceptor terminals with their freely floating ribbons. The right panel of Fig. 2 summarizes the results of this mutant screen. Although Piccolo, KIF3A, and RIM1 colocalized with RIBEYE in the mutant photoreceptor terminals, the proteins RIM2, Munc13-1, the Ca^{2+} channel α1 subunit, and ERC2/CAST1 did not. Of note, RIM2 and the Ca^{2+} channel α1 subunit colocalize at hot spots in the mutant photoreceptor terminals, but not RIM1 and RIM2 (unpublished data). It should be pointed out that the appearance of the photoreceptor ribbons labeled for RIBEYE changes from a horseshoe shape in the wild-type photoreceptor terminals (Fig. 2, left) to immunoreactive puncta of variable size in the mutant photoreceptor terminals (Fig. 2, right).

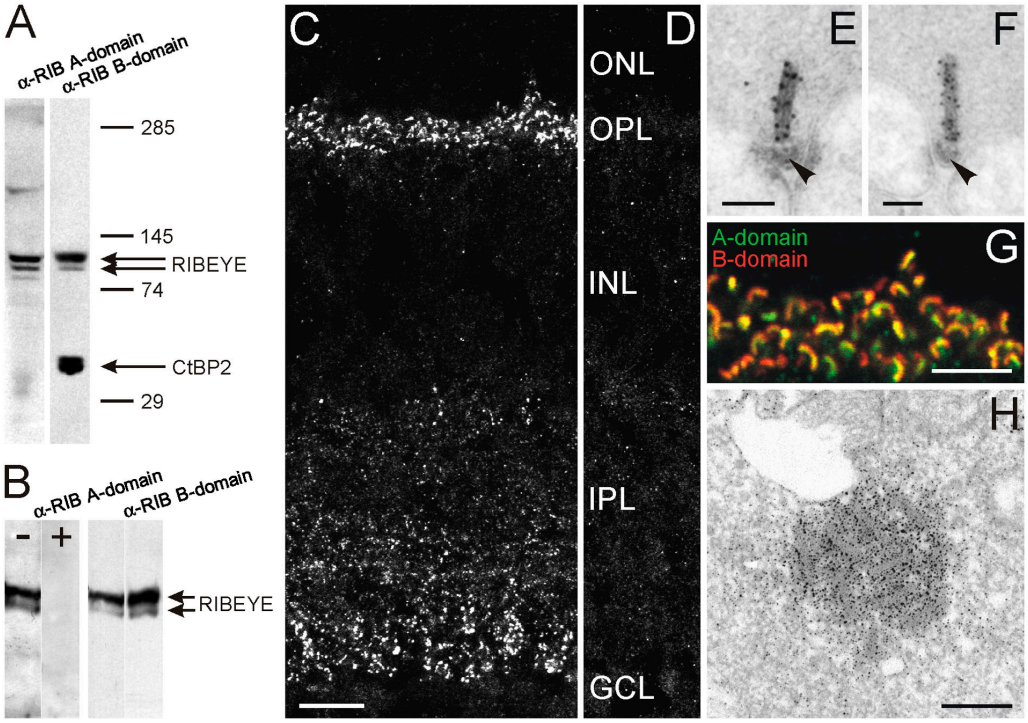

Figure 1. **Characterization of the photoreceptor ribbon protein RIBEYE in wild-type and Bassoon mutant mice.** (A) Immunoblot of mouse retinal homogenate probed with antibodies against RIBEYE A- and B-domain. Two protein bands (double arrow) of ~110 kD and 120 kD, representing RIBEYE, are recognized by both antibodies. In addition, the anti-RIBEYE B-domain antibody labels the 50-kD CtBP2 protein band (arrow). Protein bands above and below the RIBEYE doublet are unspecific and appeared only occasionally. (B) Preincubation of the anti-GST-RIBEYE A-domain antiserum with an excess of the MBP-RIB179-448 fusion protein (+) completely prevents the immunodetection of RIBEYE. −, no RIBEYE antigen included. Incubation of the same blot with the anti-RIBEYE B-domain antibody shows the presence of RIBEYE in both lanes. (C) In a vertical cryostat section through mouse retina, the anti-RIBEYE A-domain antiserum stains the photoreceptor ribbons in the outer plexiform layer (OPL) and the bipolar cell ribbons in the inner plexiform layer (IPL). (D) Preadsorption of the anti-RIBEYE antiserum with the antigen results in a complete loss of RIBEYE staining. (E and F) EM and postembedding immunogold labeling shows that photoreceptor ribbons are decorated with gold particles for RIBEYE A- (E) and B-domain (F). Note the absence of gold particles at the base of the ribbons (arrowheads), the region of the arciform density. (G) Confocal laser-scanning micrograph of a region of the OPL double labeled for RIBEYE A- (green) and B-domain (red) demonstrate the colocalization of the two immunoreactivities at the photoreceptor ribbons. (H) An aggregate of free-floating ribbons in a cone photoreceptor terminal of Bassoon mutant retina decorated with RIBEYE immunoreactivity (preembedding labeling). ONL, outer nuclear layer; INL, inner nuclear layer; GCL, ganglion cell layer. Bars: 10 μm (C and D); 0.1 μm (E and F); 5 μm (G); and 0.4 μm (H).

A likely reason could be that, although the size of mutant and wild-type ribbons appears similar in single ultrathin sections, the three-dimensional extension of the mutant ribbons is smaller. The large immunoreactive puncta represent aggregates of several free ribbons in mutant cone photoreceptor terminals, the small immunoreactive puncta are single free ribbons in mutant rod photoreceptor terminals (Fig. 1 H, 2). Furthermore, in the mutant photoreceptor terminals, staining became more diffuse for RIM2, Munc13-1, the Ca^{2+} channel α1 subunit, and ERC2/CAST1.

To examine if the differential localization of CAZ proteins within the synaptic ribbon complex observed in Bassoon mutants reflects the wild-type situation, postembedding immunogold localization analyses were performed on wild-type retina. Gold particles for RIM1 are distributed in regularly spaced clusters along the whole length of the photoreceptor ribbon (Fig. 3, A and B) and the gold particles for KIF3A are evenly distributed along the photoreceptor ribbon (Fig. 3, C and D). For both proteins the arciform density is devoid of gold particles, which is also found for the distribution of Piccolo at the ribbon (Dick et al., 2001). In contrast, the Ca^{2+} channel α1 subunit is precisely localized to the plasma membrane at the active zone (Fig. 3, E and F, arrowheads), and the gold particles for Bassoon are located to the base of the ribbon (see Fig. 6; Brandstätter et al., 1999). These findings at wild-type photoreceptor ribbon synapses support our light microscopical findings of proteins associated with the ribbon, viz Bassoon, Piccolo, RIM1, and KIF3A, and of proteins associated with the presynaptic plasma membrane/arciform density, viz RIM2, Munc13-1, a Ca^{2+} channel α1 subunit, and ERC2/CAST1.

RIBEYE interacts with wild-type Bassoon

The Bassoon mutant phenotype suggests that interactions of Bassoon with its natural binding partners are involved in the assembly of the ribbon structure. Therefore, we immunoprecipitated and analyzed Bassoon protein complexes from wild-type retina. Our immunoblot analyses revealed that large amounts of RIBEYE, Piccolo, and ERC2/CAST1 were coimmunoprecipitated specifically with Bassoon (Fig. 4 A). Control IgG did not precipitate these proteins (Fig. 4 A). Only very low amounts of RIM1/2 and Munc13-1 coimmunoprecipitated with Bassoon as observed upon long exposition of the blots shown in Fig. 4 A (unpublished data). The cell adhesion molecule cadherin (Fig.

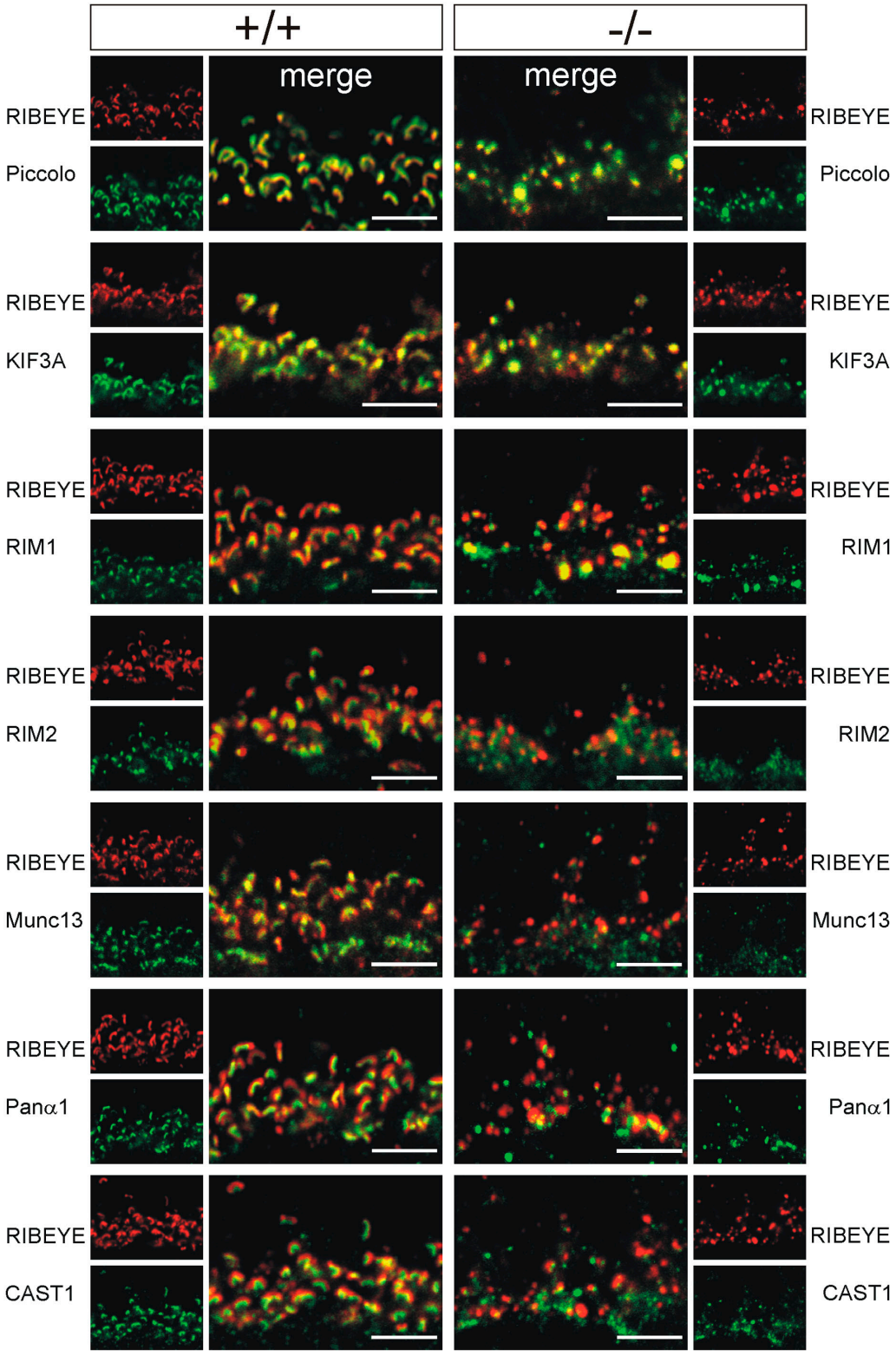

Figure 2. **Screening the photoreceptor ribbon synaptic complex for ribbon-associated proteins in wild-type (+/+) and Bassoon mutant (−/−) retinae.** (Left) Confocal laser-scanning micrographs of photoreceptor ribbons in the +/+ retina double labeled for RIBEYE combined with the following CAZ proteins: Piccolo, KIF3A, RIM1, RIM2, Munc13-1, Ca^{2+} channel α1 subunit, and ERC2/CAST1. All CAZ proteins colocalize with RIBEYE as seen in the merge of the stainings. (Right) In the −/− retina, Piccolo, KIF3A, and RIM1 colocalize with RIBEYE, but not RIM2, Munc13-1, Ca^{2+} channel α1 subunit, and ERC2/CAST1. Bars, 5 μm.

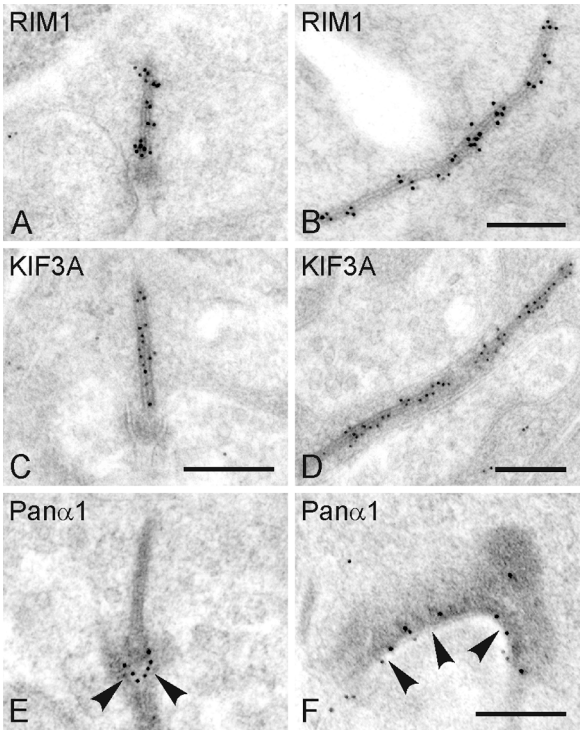

Figure 3. **Postembedding immunogold localization of CAZ proteins at wild-type photoreceptor ribbons.** Electron micrographs showing different planes of section through photoreceptor ribbons that are postembedding immunogold labeled for RIM1 (A and B), KIF3A (C and D), and a Ca^{2+} channel α1 subunit (E and F). The gold particles for RIM1 and KIF3A are associated with the ribbon, the gold particles for the Ca^{2+} channel α1 subunit are associated with the active zone at the ribbon (arrowheads). Bars, 0.2 μm.

4 A), the Ca^{2+} channel α1 subunit (unpublished data), and the kinesin motor protein KIF3A (see Fig. 6 F) were not coimmunoprecipitated with Bassoon. There was also no immunoprecipitation of the polyphosphoinositide phosphatase synaptojanin 1 (see Fig. 6 F), which was recently shown to be the protein mutated in the zebrafish nrc mutant that displays a photoreceptor phenotype similar, although not completely identical, to the Bassoon mutant phenotype (Van Epps et al., 2004).

The identification of RIBEYE in the immunoprecipitated Bassoon complexes prompted us to investigate the putative Bassoon–RIBEYE interaction more closely because RIBEYE, in contrast to Piccolo and ERC2/CAST1, is specific for ribbon synapses (Schmitz et al., 2000). Our hypothesis of a Bassoon–RIBEYE interaction was strongly supported by yeast two-hybrid experiments that were performed in parallel in order to identify Bassoon binding partners that specifically interact with the central part of Bassoon that is lacking in Bassoon mutant mice. A screen conducted with the bait RB29 on a rat brain cDNA library revealed the RIBEYE homologue CtBP1 as potential binding partner for Bassoon (Fig. 4 B). As CtBP1 shows strong homologies to RIBEYE, both interactions were studied in more detail. Subclones of RB29 were generated and tested for their interaction with CtBP1 as well as with the A- and B-domain of RIBEYE. As documented in Fig. 4 B, a region situated between the coiled-coil (CC) regions 1 and 2 of Bassoon encoded by clones RB29, RB35, and RB46 (aa 1653–2087) are able to interact with both CtBP1 and the RIBEYE B-domain, but not with the RIBEYE A-domain. No other regions of Bassoon seem to interact with CtBP1 and RIBEYE (Fig. 4 B). These data demonstrate that the interaction of RIBEYE and CtBP1 with Bassoon is mediated by a region that is missing in the mutant protein, and therefore might contribute to the observed phenotype of freely floating photoreceptor ribbons in mutant mice.

Reconstitution of RIBEYE B-domain/GFP-Bassoon interaction upon heterologous expression

To confirm the results from the yeast two-hybrid analysis and the immunoprecipitation experiment of an interaction between

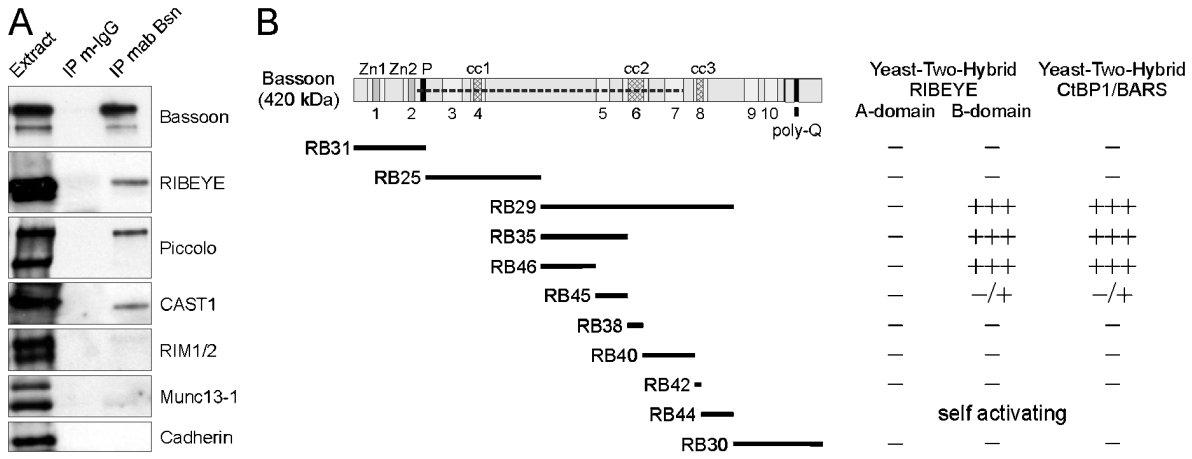

Figure 4. **Biochemical and yeast two-hybrid analysis of the Bassoon interaction with members of the CtBP family.** (A) Immunoblots showing that Bassoon complexes containing RIBEYE, Piccolo, and ERC2/CAST1 can be coimmunoprecipitated from wild-type retina extracts with a monoclonal anti-Bassoon antibody. Under the conditions used, no considerable amounts of RIM1/2, Munc13-1, and cadherin are detectable in immunoprecipitates. (B) Yeast two-hybrid analysis shows strong binding of Bassoon constructs harboring aa 1653–2087 (fragments RB29, RB35, RB46) with the RIBEYE B-domain and the RIBEYE homologue CtBP1. Construct RB45 shows only a weak interaction; construct RB44 is self activating. Specificity of the binding is shown by the lack of binding to the RIBEYE A-domain. –, no reporter gene activation; –/+, weak reporter gene activation; +++, strong reporter gene activation. Zn1, Zn2: double zinc fingers; cc1, cc2, cc3: coiled-coil domains; poly-Q: polyglutamine stretch. Numbers indicate Piccolo–Bassoon homology regions 1–10; dashed line indicates the region of Bassoon missing in the mutant protein.

a central region of Bassoon and the RIBEYE B-domain, we examined the ability of Bassoon and RIBEYE to interact upon heterologous expression in COS cells.

The RIBEYE B-domain was targeted to the outer mitochondrial membrane by generating a fusion construct with an appropriate mitochondrial targeting sequence and a flag epitope tag (Mito-RIB-B). The construct is successfully localized to mitochondria as indicated by costaining with anti-Flag antibodies and MitoTracker (Fig. 5, A–C). A clear ring-like structure of the anti-Flag immunostaining (green) encircling mitochondria (red) suggests that the RIBEYE construct is successfully targeted to mitochondria and inserted in a correct orientation into the outer mitochondrial membrane (Fig. 5 C, inset).

Next, we analyzed the cellular distribution of GFP-Bassoon constructs in single transfection experiments. Most of the GFP-Bassoon constructs tested were diffusely distributed and not associated with mitochondria as exemplified for the GFP-RB46 construct in Fig. 5, D–F (compare with Fig. 4 B for extension of constructs). Some signal was also observed in the nucleus (Fig. 5 D).

When cells were cotransfected with GFP-RB46 and Mito-RIB-B (Fig. 5, G–J), GFP-RB46 localization clearly overlapped with that of Mito-RIB-B. The cytosol and the nuclei of double-transfected cells were devoid of any GFP-RB46 (Fig. 5, G–J), suggesting that the interaction with RIBEYE is of high affinity. Similar results were obtained with a more extended GFP-Bassoon fusion protein construct, GFP-RB35 (unpublished data).

Parts of Bassoon that showed no binding in the yeast two-hybrid analysis, such as RB40, maintained their diffuse distribution in both the cytosol and the nucleus when cotransfected with Mito-RIB-B. The GFP-RB45 construct, which includes a region of Bassoon that displayed very weak interaction in the yeast two-hybrid analyses, also did not adopt the mitochondrial distribution pattern when cotransfected with Mito-RIB-B (Fig. 5, K–M).

Reverse experiments with the GFP-RIBEYE B-domain, which shows a diffuse distribution when transfected alone, cotransfected into cells expressing the RB35 fused with mito-targeting sequences, confirmed the formation of Bassoon–RIBEYE complexes. In contrast, the Bassoon domains of RB40 and RB45 fused to a mitochondrial targeting sequence failed to recruit the GFP-RIBEYE B-domain (unpublished data).

These data clearly confirm that the domains of Bassoon encoded by RB35 and RB46 interact with RIBEYE in living cells, whereas those encoded by RB40 and RB45 do not.

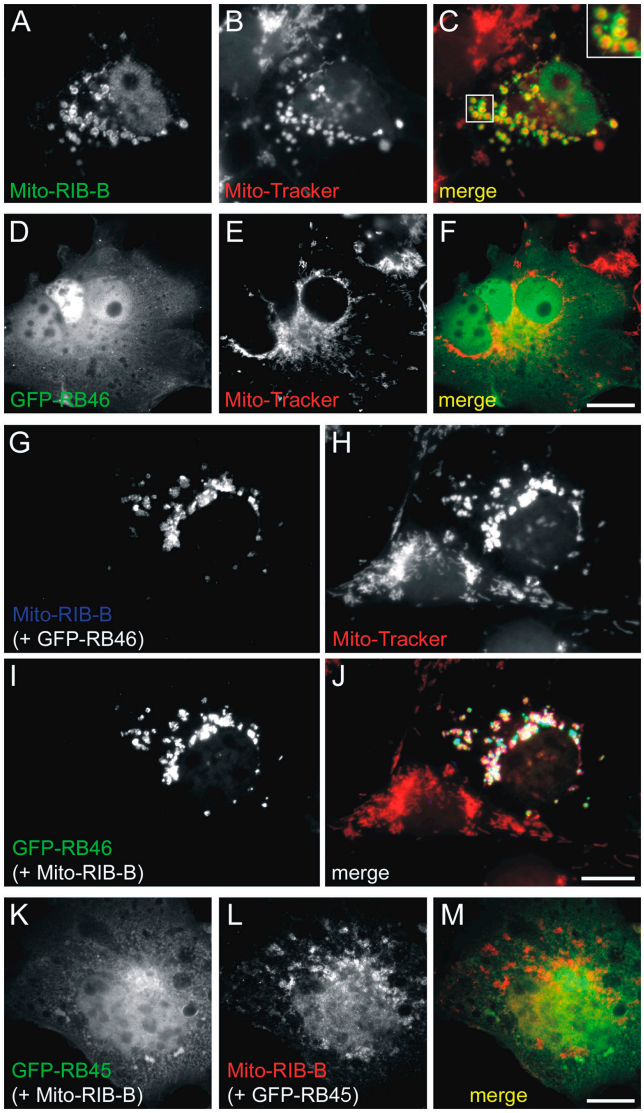

Figure 5. **Reconstitution of Bassoon–RIBEYE protein complexes by cotransfection of the Bassoon and RIBEYE binding domains in COS cells.** (A–C) Mito-RIBEYE B-domain constructs (A; anti-flag immunosignal) localize to mitochondria (B; MitoTracker Red CMXRos), best seen in the inset in the merge of the two stainings in C. (D–F) The GFP-RB46 (D) construct is distributed diffusely when expressed alone and shows no similarity in pattern with mitochondria (E and F). (G–J) In double-transfection experiments with the Mito-RIB-B-domain, the GFP-RB46 construct (I) adopts a pattern that overlaps with that of the Mito-RIB-B-domain (G) and the MitoTracker (H), as clearly seen when images are merged (J). (K–M) In contrast, the GFP-RB45 construct (K) remains diffusely distributed and shows no enrichment at mitochondria in cells that are cotransfected with the Mito-RIB-B-domain (L), as seen in the merge of the two stainings (M). Bars, 10 μm.

Interaction of Bassoon and RIBEYE at the base of the ribbon

With immunocytochemistry and light and electron microscopy we examined in detail the expression patterns of Bassoon and RIBEYE at the photoreceptor ribbon synapses. In light microscopy, the immunoreactivities of the two proteins overlap in a horseshoe shape, with RIBEYE (Fig. 6 A, red) surrounding Bassoon (Fig. 6 B, green) as seen in the merge of the two stainings (Fig. 6 C). This finding is corroborated by the results from double-labeling postembedding immunogold experiments, in which we combined staining for Bassoon and RIBEYE using gold particles of different size (20 nm for Bassoon, 10 nm for RIBEYE). Fig. 6 D shows two different planes of section through photoreceptor ribbon synapses. One plane is parallel to the extent of the active zone (en face view), the other is orthogonal to it (cross-section view; Fig. 6 D, inset). Consistent with a previous quantitative examination of the localization of Bassoon (Dick et al., 2001), in both cases the larger gold particles for Bassoon are located closest to the active zone (Fig. 6 D, arrowheads). Together, these findings suggest a physical interaction between Bassoon and RIBEYE at the base of the photoreceptor ribbon.

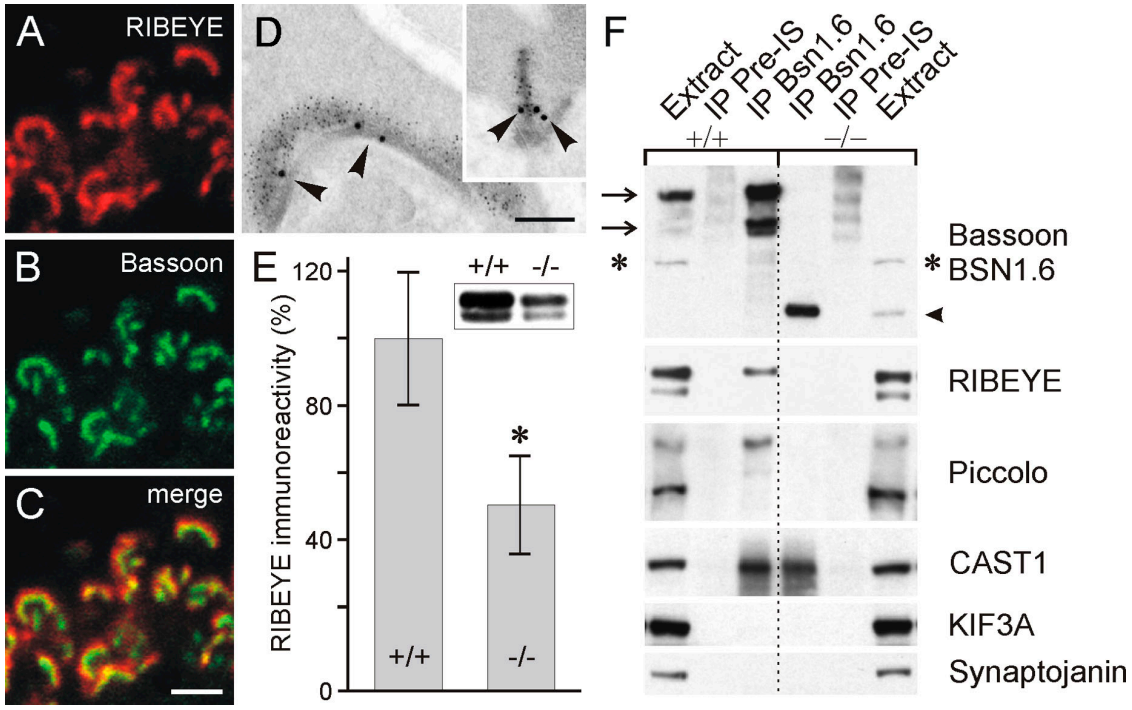

Figure 6. **Bassoon–RIBEYE interaction at the base of the photoreceptor ribbon.** (A–C) Confocal laser-scanning micrographs of photoreceptor ribbon synapses double labeled for RIBEYE (A) and Bassoon (B). In the merge of the two stainings (C), the horseshoe-like appearance of the photoreceptor ribbon colabeled for RIBEYE and Bassoon is clearly visible. Bassoon labeling is surrounded by the RIBEYE labeling. (D) Electron micrographs of photoreceptor ribbons, en face and cross-section view (inset), postembedding immunogold double labeled for Bassoon (large gold particles) and RIBEYE (small gold particles). The gold particles for Bassoon are located closest to the active zone (arrowheads). (E) Immunoblots of 25 μg total protein per lane from wild-type (+/+) and Bassoon mutant (−/−) retina homogenates show a 50% reduction of RIBEYE immunoreactivity in the −/− retina. Data are normalized to the mean value (100%) obtained from wild-type samples. Statistical analysis by the unpaired *t* test shows a significant difference in the RIBEYE immunoreactivity between the two genotypes (asterisk, $P < 0{,}01$). Results are expressed as mean ± SD; $n = 4$ for both genotypes. (F) Immunoprecipitation experiments from wild-type (+/+) and mutant (−/−) retinal extracts with the rabbit antiserum BSN1.6 directed against the NH_2-terminal part of wild-type and mutant Bassoon. The arrows on the left indicate wild-type Bassoon (420 and 320 kD), the arrowhead on the right indicates the 180-kD mutant protein. Note that the unspecific band (asterisk) is not precipitated. RIBEYE is coimmunoprecipitated from wild-type but not from Bassoon mutant retina. The same is true for the higher molecular weight band of Piccolo. In contrast, ERC2/CAST1 is found in both precipitates. Kinesin KIF3A and synaptojanin are not detected in either precipitate. Control experiments were performed with preimmune serum (preIS). IP, immunoprecipitation. Bars: 2 μm (A–C), 0.2 μm (D).

The region of Bassoon that interacts with RIBEYE is missing in the 180-kD Bassoon mutant protein ($Bsn^{\Delta Ex4/5}$), which is still made in the Bassoon mutant mouse (Altrock et al., 2003), but it is not targeted to the active zone and is diffusely distributed throughout the photoreceptor terminals (Dick et al., 2003). As the interaction between Bassoon and RIBEYE should be absent in mutant mice, we examined if RIBEYE expression and distribution is affected in mutant retinae. As shown in Fig. 6 E, the overall amount of RIBEYE in the Bassoon mutant retina is reduced to about half (52% ± 14%) as compared with wild-type retina (100% ± 19%). To confirm that mutant Bassoon protein does not bind to RIBEYE, we performed immunoprecipitation experiments with an antibody against the NH_2-terminal region of Bassoon (BSN1.6), which recognizes both wild-type and mutant Bassoon (Fig. 6 F). This antibody coimmunoprecipitated RIBEYE, Piccolo, and ERC2/CAST1 but not KIF3A or synaptojanin from wild-type retina extracts (Fig. 6 F). In contrast, only ERC2/CAST1 but not RIBEYE and Piccolo was coprecipitated from mutant retina extracts (Fig. 6 F). This finding is consistent with the absence of the RIBEYE-binding site in mutant Bassoon, whereas the binding site for ERC2/CAST1, which was mapped to the CC3 domain (aa 2933–2995 of wild-type Bassoon; Takao-Rikitsu et al., 2004) is still present in the mutant protein.

The RIBEYE B-domain homologue CtBP1 is present at ribbon and conventional synapses

As the interaction of Bassoon was originally observed with CtBP1, a homologue of the RIBEYE B-domain, we monitored the distribution of this protein in vertical sections of wild-type mouse retina using a monoclonal mouse anti-CtBP1 antibody. Interestingly, in addition to the expected nuclear staining, strong CtBP1 labeling was observed in the two synaptic layers of the retina (Fig. 7 A). Double-labeling experiments with an antiserum against the CAZ protein Piccolo, which is present at ribbon and conventional synapses in the retina (Fig. 7 B; Dick et al., 2001), show a complete colocalization of CtBP1 and Piccolo in the two plexiform layers of the retina (Fig. 7 C). Postembedding immunogold EM further proved the presence of CtBP1 at ribbon and conventional synapses in the retina (Fig. 7, D and E). Immunoblot analysis revealed no cross-reactivity of the CtBP1 antibody with RIBEYE (Fig. 7 F), demonstrating

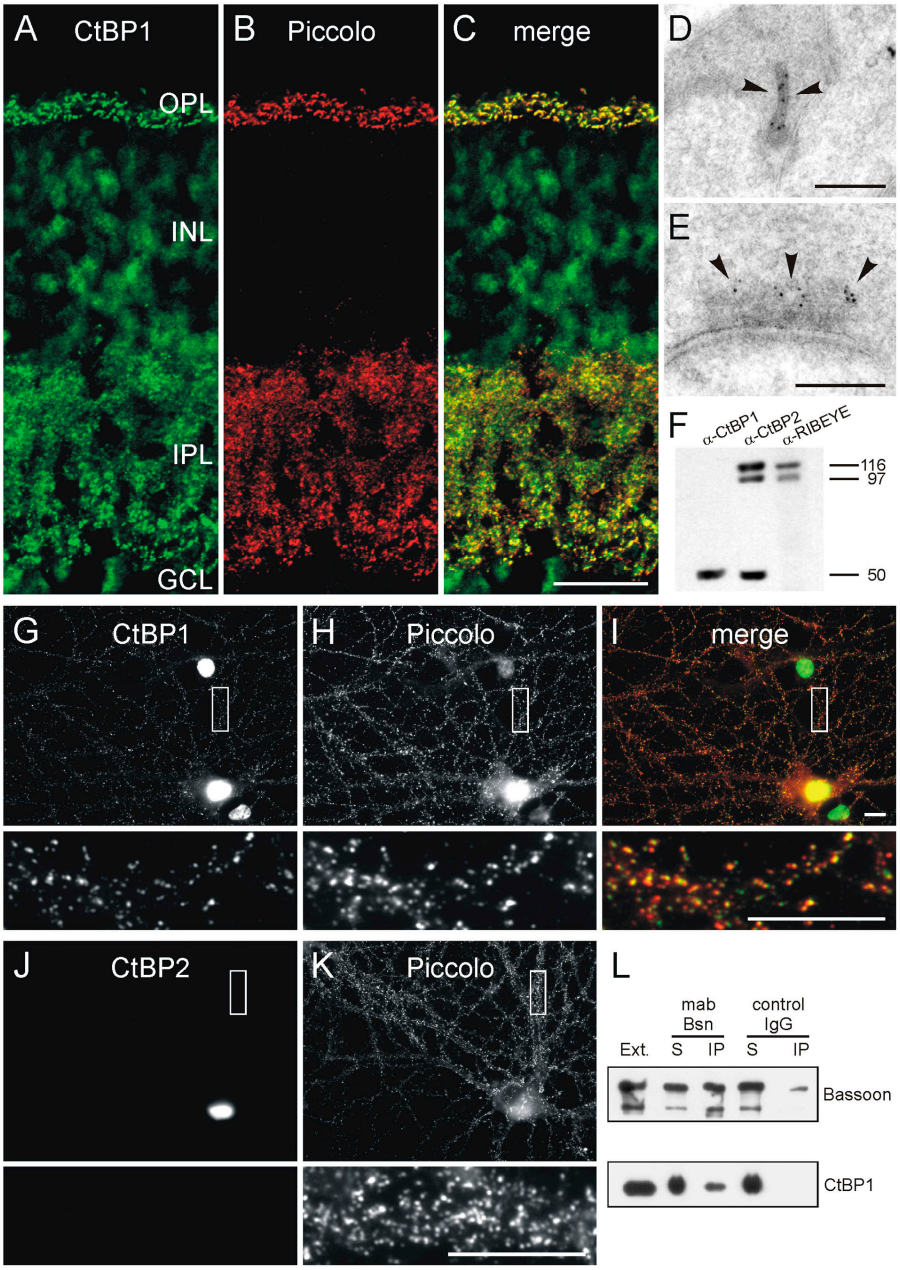

Figure 7. **CtBP1, a RIBEYE homologue, is expressed at ribbon and conventional synapses.** (A–C) Confocal laser-scanning micrographs of a vertical section through mouse retina double labeled for CtBP1 (A) and Piccolo (B), which marks ribbon and conventional synapses in the retina. As seen in the merge of the two stainings (C), CtBP1 and Piccolo immunoreactivities completely colocalize at the synapses in the outer plexiform layer (OPL) and inner plexiform layer (IPL) of the retina. (D and E) Electron micrographs of a photoreceptor (D) and an amacrine cell synapse (E) immunogold labeled for CtBP1. At the ribbon synapse the gold particles for CtBP1 decorate the ribbon (arrowheads), at the amacrine cell synapse they are located some distance from the active zone (arrowheads) at the edge of the electron-dense CAZ material. (F) Western blots of retina homogenate probed with antibodies against CtBP1 and the RIBEYE A- and CtBP2/RIBEYE B-domain. The antibody against CtBP1 recognizes the 50-kD CtBP1 protein and does not cross-react with RIBEYE. (G–I) Micrographs of cultured hippocampal neurons double labeled for CtBP1 (G) and Piccolo (H). In hippocampal neurons, like in retinal neurons, a fraction of CtBP1 immunoreactivity is localized at synapses where it colocalizes with Piccolo as seen in the merge of the two stainings (I). (J and K) CtBP2 (J) is not present at hippocampal synapses labeled with Piccolo (K). (L) Immunoblots showing that CtBP1 can be coimmunoprecipitated from brain synaptosomes with a monoclonal anti-Bassoon antibody. The boxes in G–K mark the regions that are shown at higher magnification. INL, inner nuclear layer; GCL, ganglion cell layer; Ext., brain synaptosomal extract; IP, immunoprecipitate; S, supernatant. Bars: 20 μm (A–C), 0.2 μm (D and E), and 10 μm (G–K).

that indeed the 50-kD CtBP1 protein is present synaptically. In the Bassoon mutant photoreceptor terminals with their free-floating ribbons, CtBP1 stays associated with RIBEYE (unpublished data), adding CtBP1 to the list of potential interactors with the photoreceptor ribbon.

Although RIBEYE is specific for ribbon synapses, CtBP1 is also present at conventional synapses in the retina. This raised the question whether brain synapses also express members of the CtBP family. Indeed, double-labeling experiments with Piccolo on primary cultures from hippocampal neurons demonstrate the presence of CtBP1 but the absence of CtBP2 at hippocampal synapses (Fig. 7, G–K). Like RIBEYE at ribbon synapses, CtBP1 seems to interact with Bassoon at conventional synapses because it can be coimmunoprecipitated with Bassoon from brain synaptosomal fractions (Fig. 7 L).

Discussion

Photoreceptor cells, the primary neurons of the retina, are non-spiking neurons that use graded changes in membrane potential to transmit sensory information over a wide dynamic range of light intensities. The continuous adjustment of the synaptic output to changes in the incoming signals requires a specialized type of synapse, the ribbon synapse, that sustains high and long-lasting rates of neurotransmitter release (von Gersdorff, 2001; Parsons and Sterling, 2003).

The photoreceptor ribbon complex is subdivided into two molecular compartments

Photoreceptor ribbon synapses exocytose hundreds of vesicles per second, which requires a large pool of readily releasable

vesicles and a fast release mechanism. The current hypothesis of calcium-dependent exocytosis at retinal ribbon synapses suggests that (1) the vesicles tethered to the ribbon are primed; (2) the vesicles that are in closest contact with the presynaptic plasma membrane at the ribbon base comprise the small, rapidly releasable pool of vesicles; and (3) the remaining vesicles tethered to the ribbon comprise the large, readily (slower) releasable pool (von Gersdorff et al., 1996; Heidelberger et al., 2002; Parsons and Sterling, 2003).

The ultrastructural appearance of a row of synaptic vesicles tethered to either side of the ribbon and the expression of a kinesin motor protein KIF3A at retinal ribbon synapses (Muresan et al., 1999) led to the conceptually attractive model that the ribbon, like a conveyor belt, moves primed vesicles to the docking/release site at the base of the ribbon. However, this model raises the question of how the whole readily releasable pool can be exocytosed within 1–2 ms, which is much too fast for moving the rows of vesicles to the release site by an active, kinesin-powered movement (Heidelberger et al., 1994). A challenging concept to explain these questions is compound exocytosis, a process by which vesicles tethered to the ribbon fuse with each other and with the vesicles docked at the plasma membrane (Parsons and Sterling, 2003). However, experimental evidence for compound fusion at ribbon or conventional chemical synapses is sparse.

Both scenarios, conveyor belt or compound fusion, postulate that membrane fusion and transmitter release occurs focally at the ribbon base. This is supported by our findings of the preferential clustering of a Ca^{2+} channel α1 subunit and Munc13-1 in addition to RIM2 and ERC2/CAST1 at the presynaptic plasma membrane/arciform density compartment. As Munc13 seems to be an essential component of the priming machinery for synaptic vesicles at conventional synapses (Rosenmund et al., 2003), it may be assumed that the final priming steps take place near the active zone membrane.

In our search for CAZ proteins that potentially interact at the photoreceptor ribbon complex, we were able to dissect a second cytomatrix compartment that is distinct from the plasma membrane/arciform density compartment, the ribbon (Fig. 8). The two compartments are likely to reflect a segregation of CAZ functions at the photoreceptor ribbon synapse. This is most obvious by the differential distribution of RIM1 and RIM2. RIMs, CAZ proteins that function in a late step of exocytosis following the docking of synaptic vesicles, directly and indirectly interact with many proteins implicated in vesicle priming and neurotransmitter release at presynaptic active zones of synapses, including Munc13-1, ERC2/CAST1, and L-type calcium channels (Wang et al., 1997; Schoch et al., 2002; Calakos et al., 2004; Südhof, 2004). Ribbon-associated molecules including RIM1, Piccolo, RIBEYE/CtBP2, and CtBP1 may be involved in tethering synaptic vesicles to the ribbon and in preparing them for exocytosis. In particular, the functions proposed for RIBEYE/CtBP2 and CtBP1 could play a role in this latter process. Both proteins were first characterized as transcriptional corepressors (Turner and Crossley, 2001). In addition, they display homology to NAD^+-dependent dehydrogenases and bind NAD^+/NADH (Schmitz et al., 2000; Zhang et al., 2002). Most interestingly, in the context of preparing vesicles for exocytosis at the ribbon, they may function as lysophosphatidic acyl-CoA transferases (LPAAT) and thus modulate the curvature of lipid membranes (Kooijman et al., 2003). Indeed, CtBP1 has been implicated in membrane fission processes at the Golgi complex, where it is involved in a fission reaction generating aligned vesicles from continuous tubular structures (Weigert et al., 1999). As shown in this paper, CtBP1 is not only a protein of the photoreceptor ribbon synapse, but also of conventional brain synapses. This suggests a general role for CtBP family members in active zone function. Our results add molecular evidence to the hypothesis that the ribbon has a correlate at the conventional synapse (Zhai and Bellen, 2004).

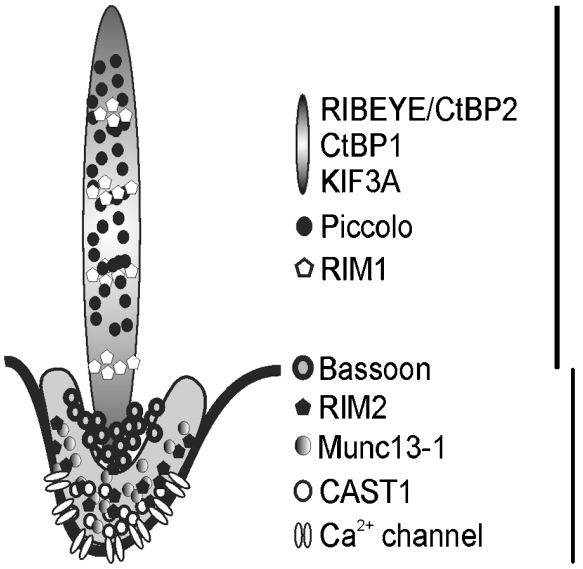

Figure 8. **Differential localization of CAZ proteins defines two compartments of the photoreceptor ribbon synaptic complex.** The ribbon-associated complex of CAZ proteins includes RIBEYE/CtBP2, CtBP1, KIF3A, Piccolo, and RIM1; the plasma membrane/arciform density-associated complex includes RIM2, Munc13-1, ERC2/CAST1, and a Ca^{2+} channel α1 subunit. Bassoon localizes at the border between the two compartments.

Bassoon, a physical link between the two CAZ compartments at the photoreceptor ribbon synapse

The floating ribbon phenotype in Bassoon-deficient retina suggests a functional involvement of Bassoon in anchoring the ribbon to the active zone (Dick et al., 2003). One possible explanation for this phenotype is that due to the lack of functional Bassoon, ribbon assembly is disturbed and/or delayed and therefore an appropriate anchoring is impossible. Data presented here offer a more precise explanation: Bassoon might be involved in linking the two newly identified compartments of the ribbon complex, i.e., the ribbon itself and the presynaptic plasma membrane/arciform density compartment. Immunogold data show that Bassoon is localized right at the border between the two CAZ compartments. At least two molecular interactions will be relevant for the attachment of the ribbon to the presynaptic plasma membrane—one interaction linking Bassoon to the synaptic ribbon, and one linking Bassoon to the plasma membrane.

Here, we show that Bassoon directly binds and functionally interacts with RIBEYE, the protein postulated to serve as a central building block of the synaptic ribbon (Schmitz et al., 2000). The cotransfection experiments in mammalian cells in vivo show a strong interaction between Bassoon and RIBEYE, and demonstrate that the interaction domains found by yeast two-hybrid analysis are sufficient for the interaction of the two proteins. The domain in Bassoon responsible for establishing the connection with RIBEYE is lost in the mutant Bassoon protein, and consequently the interaction between the two proteins. Currently, we do not know what the link is between Bassoon and the arciform density/plasma membrane compartment. A likely candidate is ERC2/CAST1, which has been shown to directly interact with Bassoon (Takao-Rikitsu et al., 2004) and which is present at the photoreceptor ribbon synapse (this paper). Because the interaction sites for ERC2/CAST1 and RIBEYE map to different locations on Bassoon (ERC2/CAST1, Takao-Rikitsu et al., 2004; RIBEYE, this paper), a simultaneous binding of the two proteins to Bassoon is possible. We propose that Bassoon contributes essentially to the link between the two compartments at the photoreceptor ribbon complex. The loss of the Bassoon–RIBEYE interaction explains the phenotype of free-floating photoreceptor ribbons in the Bassoon mutant retina.

Materials and methods

All animal experiments were performed in compliance with the guidelines for the welfare of experimental animals issued by the Federal Government of Germany, the National Institutes of Health, and the Max Planck Society. Mice were used at an age of 7–9 wk.

Antibodies

The following primary antibodies were used: mouse anti-CtBP1 (postembedding immunoelectron microscopy [post-EM] 1:500; immunohistochemistry [IHC] 1:2,500–1:5,000; Western blot [WB] 1:5,000) and anti-CtBP2 mAbs (post-EM 1:1,000; IHC 1:10,000; WB 1:5,000; BD Biosciences), rabbit anti-pan-Munc13 pAb (WB 1:250; BD Biosciences), mouse anti-RIM mAb (WB 1:1,000; BD Biosciences), rabbit anti-RIM1 (post-EM 1:50; IHC 1:500) and anti-RIM2 pAbs (IHC 1:500; Synaptic Systems GmbH), rabbit anti-synaptojanin pAb (WB 1:3,000; Synaptic Systems GmbH), rabbit anti-ERC1b/2 pAb (WB 1:5,000; Synaptic Systems GmbH), mouse anti-Bassoon mAb (IHC 1:2,500; WB 1:1,000; StressGen Biotechnologies), rabbit anti-Bassoon pAb sap7f (post-EM 1:800; tom Dieck et al., 1998), mouse anti-Flag M2 mAb (IHC 1:1,000; Sigma-Aldrich), mouse anti-pan cadherin mAb (WB 1:100; a gift of Dr. P. Beesley, Royal Holloway University London, Egham, Surrey, UK), rabbit anti-pan α1 Ca^{2+} channel pAb (post-EM 1:50; IHC 1:100; Alomone Labs), mouse anti-kinesin II mAb (post-EM, IHC 1:50; WB 1:2,000; BAbCo), guinea pig anti-Piccolo (IHC 1:8,000; WB 1:1,000–1:2,000) and rabbit anti-Piccolo pAbs (IHC 1:400; Dick et al., 2001), and mouse anti-Munc13-1 mAb (IHC 1:800; a gift of Dr. N. Brose, Max Planck Institute for Experimental Medicine, Göttingen, Germany).

Furthermore, rabbit antisera were produced against bacterially expressed GST fusion proteins of Bassoon (aa 73–181; BSN1.6), ERC2/CAST1 (aa 73–185), and RIBEYE (aa 179–48).

Retinal tissue preparation and light and electron microscopic immunocytochemistry

A description of the preparation of the retinal tissue for light and electron microscopic immunocytochemistry is given in Dick et al. (2001). For light microscopy, retinae were fixed in 4% PFA in phosphate buffer (0.1 M, pH 7.4) for 15–30 min. For postembedding immuno-EM fixation was in 0.5% glutaraldehyde and 4% PFA in phosphate buffer for 2 h.

Retinal sections were incubated in primary antibodies overnight. For light microscopy, secondary antibodies were coupled to Alexa 594, 488, or 350 (1:500; Molecular Probes, Inc.); for postembedding immuno-EM, secondary antibodies were coupled to 10- or 20-nm gold particles (ICN Biomedicals).

For light microscopic analysis, labeled sections were examined with a confocal laser-scanning microscope (LSM5 Pascal; Carl Zeiss MicroImaging, Inc.). Images were adjusted for contrast and brightness using Adobe Photoshop version 5.5, and figures were arranged using Corel Draw 9. For postembedding immuno-EM, ultrathin sections were examined and photographed with an electron microscope (EM10; Carl Zeiss MicroImaging, Inc.) on negative film.

Western blot and immunoprecipitation

For Western blots of retina homogenate, retinae were homogenized, total protein was precipitated with TCA, dissolved in sample buffer, separated on 3.5–8% Tris acetate gels (25 μg/lane), and transferred to PVDF membranes by tank blotting (Altrock et al., 2003). For immunodetection, membranes were blocked and primary antibodies were applied overnight at 4°C. For characterization of the RIBEYE antiserum, 5 μl RIBEYE serum was preincubated for 1 h with an excess of purified MBP-RIB (aa 179–448) fraction or with buffer alone and then diluted for overnight incubation of the Western blots. The HRP-coupled secondary antibodies were visualized by chemiluminescent detection (Amersham Biosciences).

Blots were reprobed several times with different antibodies. Evaluation of relative amounts of RIBEYE immunoreactivity was performed by determining gray values in nonsaturated expositions of X-ray films in a given area using Adobe Photoshop for four individual +/+ and −/− animal pairs. The mean value of the +/+ animals was defined as 100%.

For immunoprecipitation experiments, retinae were homogenized in 1 ml extraction buffer (50 mM Tris-HCl, pH 7.5, 150 mM NaCl, 1% Triton X-100, and 0.5% sodium deoxycholate) per animal. Insoluble material was pelleted. For antibody immobilization, protein G–Agarose beads (25 μl bed volume; Roche) were incubated overhead (for 1 h at 4°C) with 10 μg monoclonal Bassoon antibody and as control 10 μg mouse IgG (Sigma-Aldrich), or with 5 μl rabbit anti-BSN1.6 antiserum and 5 μl of a preimmune serum as control followed by washes. The extract corresponding to one retina was applied overnight to the antibody-coupled beads. Bound proteins were recovered after extensive washes in homogenization buffer by boiling in sample buffer. Extracted material (input) and unbound proteins in the supernatant were concentrated by TCA precipitation. SDS-PAGE and immunodetection were performed as described above.

For immunoprecipitation experiments from brain material, synaptosomal fractions were prepared as described previously (Phillips et al., 2001) and were extracted with detergent buffer (0.5% sodium deoxycholate, 0.1% Triton X-100, 70 mM NaCl, 25 mM Tris-HCL, pH 8.0, and total protein 0.125 μg/μl). Mouse anti-Bassoon mAb and unspecific mouse IgG (Santa Cruz Biotechnology. Inc.) were chemically coupled to Gamma-Bind Plus Sepharose (Amersham Biosciences) to abolish background derived from antibody proteins in the immunoprecipitation fraction. In detail, 20 μg IgG was incubated for 1 h with 100 μl of beads in PBS-T buffer (8.1 mM Na_2HPO_4, 1.5 mM KH_2PO_4, 2.7 mM KCl, 137 mM NaCl, and 0.1% Tween 20, pH 7.4). Beads were washed with PBS-T and with TEA buffer (0.2 M triethanolamine, pH 8.2) before incubation for 45 min at RT in coupling buffer (20 mM dimethyl pimelimidate dihydrochlorid in TEA). Beads were washed with TEA and incubated for 10 min at RT in 20 mM ethanolamine (pH 8.2). After washing with PBS-T, beads were stored in 5% BSA in PBS-T with 0.025% NaN_3 at 4°C.

For immunoprecipitation, 10 μl of antibody-coated beads washed in extraction buffer were incubated for 1 h at 4°C with 500 μl synaptosomal extract. After washing, bound proteins were eluted with sample buffer without reducing agent for 5 min at 60°C. The eluate was incubated for 5 min at 90°C in the presence of 50 mM dithiothreitol as a reducing agent. SDS-PAGE and immunodetection were performed as described above.

DNA constructs

Bassoon fragments RB25 (aa 609–1692), RB29 (aa 1692–3263), RB30 (aa 3263–3938), and RB31 (aa 1–609) were obtained by restriction enzyme digestion of a full-length rat Bassoon cDNA plasmid (Dresbach et al., 2003). Bassoon fragments RB35 (aa 1653–2348), RB38 (aa 2349–2469), RB40 (aa 2470–2928), RB42 (aa 2929–2978), RB44 (aa 2979–3263), RB45 (aa 2088–2348), and RB46 (aa 1653–2087) were generated by amplifying the corresponding regions from a full-length rat Bassoon cDNA construct by PCR. A RIBEYE fragment encoding the A domain (aa 1–563) was obtained by PCR amplification of the corresponding sequence using a rat genomic DNA as a template. Fragments encoding the B domain of RIBEYE (aa 564–988) or CtBP1 (aa 1–430) were amplified

from a rat brain Matchmaker cDNA library (CLONTECH Laboratories, Inc.) or a rat retina cDNA library provided by Dr. M.R. Kreutz (Leibniz Institute for Neurobiology, Magdeburg, Germany). PCR products were cloned into pBlueScript II SK(−) (Stratagene) and verified by sequencing.

For yeast two-hybrid analysis, Bassoon fragments were subcloned into the bait vector pGBK-T7 (CLONTECH Laboratories, Inc.) or pGBK-T7-3, a frame shift derivative generated by standard techniques. RIBEYE and CtBP1 fragments were subcloned into the prey vector pGAD-T7 (CLONTECH Laboratories, Inc.).

Plasmids encoding GFP fusion proteins of Bassoon domains were generated by subcloning fragments RB45 and RB46 into pEGFP-C2 (CLONTECH Laboratories, Inc.). The plasmid encoding a mitochondria-targeted B-domain of RIBEYE was generated by subcloning the respective cDNA fragment into the BamH1 and SalI sites of the vector MF4 (mito-flag-frame C), a frame-shift derivative of the mito-targeting vector described previously (Kessels and Qualmann, 2002).

Yeast two-hybrid experiments

For yeast two-hybrid analysis, each Bassoon bait plasmid or the empty bait vector pGBK-T7 (control) was cotransformed with the RIBEYE A-domain, B-domain, CtBP1, or the pGAD-T7 prey plasmids into AH109 (CLONTECH Laboratories, Inc.) yeast cells using standard transformation protocols. Cotransformed cells were selected by growth on leucine- and tryptophan-lacking medium and then were assayed for reporter gene expression by growth on leucine-, tryptophan-, adenine-, and histidine-lacking medium in the presence of 1 mM 3-amino-1,2,4-triazole. Growth was monitored and scored after 7 to 10 d.

Cell culture and immunofluorescence microscopy

Transfections of COS-7 cells were performed with Polyfect according to the manufacturer's instructions (QIAGEN). For mitochondrial staining, cells were incubated for 20 min with MitoTracker Red CMXRos (Molecular Probes, Inc.) at a final concentration of 200 nM in medium at 37°C, washed, and then fixed. Fixations and immunofluorescence labelings were performed according to Kessels et al. (2001). Images were recorded digitally with a fluorescence microscope (DMRD; Leica) and an Axioplan 2 microscope (Carl Zeiss MicroImaging, Inc.), and were processed using Adobe Photoshop software. Hippocampal primary cultures were prepared and processed for immunocytochemistry as described previously (tom Dieck et al., 1998).

We are grateful to Anja Staab, Gong-Sun Nam, and Walter Hofer for expert technical assistance and to V. Eulenburg for excellent mouse ordering.

This work was supported by the Deutsche Forschungsgemeinschaft SFB 269/B4 (J.H. Brandstätter), KE685/2-1 (M.M. Kessels), QU116/2-3 (B. Qualmann), and SFB 426/A1, and by the European Commission and the Fonds der Chemischen Industrie (E.D. Gundelfinger). A. Fejtova is the recipient of a fellowship from the Swiss National Fonds.

Submitted: 26 August 2004
Accepted: 13 January 2005

References

Altrock, W.D., S. tom Dieck, M. Sokolov, A.C. Meyer, A. Sigler, C. Brakebusch, R. Fässler, K. Richter, T.M. Boeckers, H. Potschka, et al. 2003. Functional inactivation of a fraction of excitatory synapses in mice deficient for the active zone protein Bassoon. *Neuron.* 37:787–800.

Brandstätter, J.H., E.L. Fletcher, C.C. Garner, E.D. Gundelfinger, and H. Wässle. 1999. Differential expression of the presynaptic cytomatrix protein Bassoon among ribbon synapses in the mammalian retina. *Eur. J. Neurosci.* 11:3683–3693.

Brose, N., K. Hofmann, Y. Hata, and T.C. Südhof. 1995. Mammalian homologues of *Caenorhabditis elegans unc-13* gene define novel family of C-domain protein. *J. Biol. Chem.* 270:25273–25280.

Calakos, N., S. Schoch, T.C. Südhof, and R.C. Malenka. 2004. Multiple roles for the active zone protein RIM1α in late stages of neurotransmitter release. *Neuron.* 42:889–896.

Cases-Langhoff, C., B. Voss, A.M. Garner, U. Appeltauer, K. Takei, S. Kindler, R.W. Veh, P. De Camilli, E.D. Gundelfinger, and C.C. Garner. 1996. Piccolo, a novel 420 kDa protein associated with the presynaptic cytomatrix. *Eur. J. Cell Biol.* 69:214–223.

Dick, O., I. Hack, W.D. Altrock, C.C. Garner, E.D. Gundelfinger, and J.H. Brandstatter. 2001. Localization of the presynaptic cytomatrix protein Piccolo at ribbon and conventional synapses in the rat retina: comparison with Bassoon. *J. Comp. Neurol.* 439:224–234.

Dick, O., S. tom Dieck, W.D. Altrock, J. Ammermüller, R. Weiler, C.C. Garner, E.D. Gundelfinger, and J.H. Brandstätter. 2003. The presynaptic active zone protein Bassoon is essential for photoreceptor ribbon synapse formation in the retina. *Neuron.* 37:775–786.

Dresbach, T., B. Qualmann, M.M. Kessels, C.C. Garner, and E.D. Gundelfinger. 2001. The presynaptic cytomatrix of brain synapses. *Cell. Mol. Life Sci.* 58:94–116.

Dresbach, T., A. Hempelmann, C. Spilker, S. tom Dieck, W.D. Altrock, W. Zuschratter, C.C. Garner, and E.D. Gundelfinger. 2003. Functional regions of the presynaptic cytomatrix protein bassoon: significance for synaptic targeting and cytomatrix anchoring. *Mol. Cell. Neurosci.* 23:279–291.

Fenster, S.D., W.J. Chung, R. Zhai, C. Cases-Langhoff, B. Voss, A.M. Garner, U. Kaempf, S. Kindler, E.D. Gundelfinger, and C.C. Garner. 2000. Piccolo, a presynaptic zinc finger protein structurally related to Bassoon. *Neuron.* 25:203–214.

Fenster, S.D., M.M. Kessels, B. Qualmann, W.J. Chung, J. Nash, E.D. Gundelfinger, and C.C. Garner. 2003. Interactions between Piccolo and the actin/dynamin-binding protein Abp1 link vesicle endocytosis to presynaptic active zones. *J. Biol. Chem.* 278:20268–20277.

Heidelberger, R., C. Heinemann, E. Neher, and G. Matthews. 1994. Calcium dependence of the rate of exocytosis in a synaptic terminal. *Nature.* 371:513–515.

Heidelberger, R., P. Sterling, and G. Matthews. 2002. Roles of ATP in depletion and replenishment of the releasable pool of synaptic vesicles. *J. Neurophysiol.* 88:98–106.

Kessels, M.M., and B. Qualmann. 2002. Syndapins integrate N-WASP in receptor-mediated endocytosis. *EMBO J.* 21:6083–6094.

Kessels, M.M., A.E. Engqvist-Goldstein, D.G. Drubin, and B. Qualmann. 2001. Mammalian Abp1, a signal-responsive F-actin-binding protein, links the actin cytoskeleton to endocytosis via the GTPase dynamin. *J. Cell Biol.* 153:351–366.

Kooijman, E.E., V. Chupin, B. de Kruijff, and K.N. Burger. 2003. Modulation of membrane curvature by phosphatidic acid and lysophosphatidic acid. *Traffic.* 4:162–174.

Muresan, V., A. Lyass, and B.J. Schnapp. 1999. The kinesin motor KIF3A is a component of the presynaptic ribbon in vertebrate photoreceptors. *J. Neurosci.* 19:1027–1037.

Ohtsuka, T., E. Takao-Rikitsu, E. Inoue, M. Inoue, M. Takeuchi, K. Matsubara, M. Deguchi-Tawarada, K. Satoh, K. Morimoto, H. Nakanishi, and Y. Takai. 2002. CAST: a novel protein of the cytomatrix at the active zone of synapses that forms a ternary complex with RIM1 and Munc13-1. *J. Cell Biol.* 158:577–590.

Parsons, T.D., and P. Sterling. 2003. Synaptic ribbon: conveyor belt or safety belt? *Neuron.* 37:379–382.

Phillips, G.R., J.K. Huang, Y. Wang, H. Tanaka, L. Shapiro, W. Zhang, W.S. Shan, K. Arndt, M. Frank, R.E. Gordon, et al. 2001. The presynaptic particle web: ultrastructure, composition, dissolution, and reconstitution. *Neuron.* 32:63–77.

Rao-Mirotznik, R., A.B. Harkins, G. Buchsbaum, and P. Sterling. 1995. Mammalian rod terminal: architecture of a binary synapse. *Neuron.* 14:561–569.

Richter, K., K. Langnaese, M.R. Kreutz, G. Olias, R. Zhai, H. Scheich, C.C. Garner, and E.D. Gundelfinger. 1999. Presynaptic cytomatrix protein Bassoon is localized at both excitatory and inhibitory synapses of rat brain. *J. Comp. Neurol.* 408:437–448.

Rosenmund, C., J. Rettig, and N. Brose. 2003. Molecular mechanisms of active zone function. *Curr. Opin. Neurobiol.* 13:509–519.

Schmitz, F., A. Königstorfer, and T.C. Südhof. 2000. RIBEYE, a component of synaptic ribbons: a protein's journey through evolution provides insight into synaptic ribbon function. *Neuron.* 28:857–872.

Schoch, S., P.E. Castillo, T. Jo, K. Mukherjee, M. Geppert, Y. Wang, F. Schmitz, R.C. Malenka, and T.C. Südhof. 2002. RIM1α forms a protein scaffold for regulating neurotransmitter release at the active zone. *Nature.* 415:321–326.

Shapira, M., R.G. Zhai, T. Dresbach, T. Bresler, V.I. Torres, E.D. Gundelfinger, N.E. Ziv, and C.C. Garner. 2003. Unitary assembly of presynaptic active zones from Piccolo-Bassoon transport vesicles. *Neuron.* 38:237–252.

Südhof, T.C. 2004. The synaptic vesicle cycle. *Annu. Rev. Neurosci.* 27:509–547.

Takao-Rikitsu, E., S. Mochida, E. Inoue, M. Deguchi-Tawarada, M. Inoue, T. Ohtsuka, and Y. Takai. 2004. Physical and functional interaction of the active zone proteins, CAST, RIM1, and Bassoon, in neurotransmitter release. *J. Cell Biol.* 164:301–311.

tom Dieck, S., L. Sanmarti-Vila, K. Langnaese, K. Richter, S. Kindler, A. Soyke, H. Wex, K.-H. Smalla, U. Kampf, J.T. Franzer, et al. 1998. Bassoon, a novel zinc-finger CAG/glutamine-repeat protein selectively localized at the active zone of presynaptic nerve terminals. *J. Cell Biol.* 142:499–509.

Turner, J., and M. Crossley. 2001. The CtBP family: enigmatic and enzymatic

transcriptional co-repressors. *Bioessays.* 23:683–690.

Van Epps, H.A., M. Hayashi, L. Lucast, G.W. Stearns, J.B. Hurley, P. DeCamilli, and S.E. Brockerhoff. 2004. The zebrafish nrc mutant reveals a role for the polyphosphoinositide phosphatase synaptojanin 1 in cone photoreceptor ribbon anchoring. *J. Neurosci.* 24:8641–8650.

Vardinon-Friedman, H., T. Bresler, C.C. Garner, and N.E. Ziv. 2000. Assembly of new individual excitatory synapses: time course and temporal order of synaptic molecule recruitment. *Neuron.* 27:57–69.

von Gersdorff, H. 2001. Synaptic ribbons: versatile signal transducers. *Neuron.* 29:7–10.

von Gersdorff, H., E. Vardi, G. Matthews, and P. Sterling. 1996. Evidence that vesicles on the synaptic ribbon of retinal bipolar neurons can be rapidly released. *Neuron.* 16:1221–1227.

Wang, X., M. Kibschull, M.M. Laue, B. Lichte, E. Petrasch-Parwez, and M.W. Kilimann. 1999. Aczonin, a 550-kD putative scaffolding protein of presynaptic active zones, shares homology regions with Rim and Bassoon and binds profilin. *J. Cell Biol.* 147:151–162.

Wang, Y., M. Okamoto, F. Schmitz, K. Hofmann, and T.C. Südhof. 1997. Rim is a putative Rab3 effector in regulating synaptic-vesicle fusion. *Nature.* 388:593–598.

Wang, Y., S. Sugita, and T.C. Südhof. 2000. The RIM/NIM family of neuronal C2 domain proteins. Interactions with Rab3 and a new class of Src homology 3 domain proteins. *J. Biol. Chem.* 275:20033–20044.

Wang, Y., X. Liu, T. Biederer, and T.C. Südhof. 2002. A family of RIM-binding proteins regulated by alternative splicing: implications for the genesis of synaptic active zones. *Proc. Natl. Acad. Sci. USA.* 99:14464–14469.

Weigert, R., M.G. Silletta, S. Spanò, G. Turacchio, C. Cericola, A. Colanzi, S. Senatore, R. Mancini, E.V. Polishchuk, M. Salmona, et al. 1999. CtBP/BARS induces fission of Golgi membranes by acylating lysophophatidic acid. *Nature.* 402:429–433.

Zhai, R.G., and H.J. Bellen. 2004. The architecture of the active zone in the presynaptic nerve terminal. *Physiology (Bethesda).* 19:262–270.

Zhai, R.G., H.V. Friedman, C. Cases-Langhoff, B. Becker, E.D. Gundelfinger, N.E. Ziv, and C.C. Garner. 2001. Assembling the presynaptic active zone: a characterization of an active zone precursor vesicle. *Neuron.* 29:131–143.

Zhang, Q., D.W. Piston, and R.H. Goodman. 2002. Regulation of corepressor function by nuclear NADH. *Science.* 295:1895–1897.

Ziff, E.B. 1997. Enlightening the postsynaptic density. *Neuron.* 19:1163–1174.